



## **Sensitivity simulation and measurement of the SKA Band 1 wideband feed package on MeerKAT**

Downloaded from: <https://research.chalmers.se>, 2026-04-05 05:04 UTC

Citation for the original published paper (version of record):

Flygare, J., Peens-Hough, A., Helldner, L. et al (2019). Sensitivity simulation and measurement of the SKA Band 1 wideband feed package on MeerKAT. 13th European Conference on Antennas and Propagation, EuCAP 2019, EuCAP 2019

N.B. When citing this work, cite the original published paper.

# Sensitivity simulation and measurement of the SKA Band 1 wideband feed package on MeerKAT

Jonas Flygare<sup>1</sup>, Adriaan Peens-Hough<sup>2</sup>, Leif Helldner<sup>1</sup>, Magnus Dahlgren<sup>1</sup>, George Smit<sup>2</sup>, Pieter Kotze<sup>2</sup>, Ronny Wingdén<sup>1</sup>, Tobia D. Carozzi<sup>1</sup>, Ulf Kylanfall<sup>1</sup>, Lars Pettersson<sup>1</sup>, Miroslav Pantaleev<sup>1</sup>

<sup>1</sup>(Onsala Space Observatory): Dept. of Space, Earth and Environment, Chalmers University of Technology, SE-41296-Gothenburg, Sweden, jonas.flygare@chalmers.se

<sup>2</sup>(SARAO): South African Radio Astronomy Observatory, Cape Town, South Africa, aph@ska.ac.za

**Abstract**—Advances in wideband feed technology for radio telescopes enable high sensitivity observations over large bandwidths. The wideband quad-ridge flared horn (QRFH) feed package for Band 1 of the Square Kilometre Array (SKA) was optimized for high sensitivity. The 3:1 feed package covers 350–1050 MHz and is a complete room temperature system with low-noise amplifiers integrated inside the ridges of the horn. The QRFH is dual-linear polarized and designed with spline-defined profiles for the horn and ridge shape. Measured feed s-parameters show input reflection less than -11 dB across the band with good port isolation. In this paper we present the first measured sensitivity levels of the Band 1 feed package, which was tested on the SKA precursor reflector MeerKAT. We also present measured aperture efficiency and intrinsic cross-polarization (IXR). The measured results show good agreement with simulations.

**Index Terms**—wideband, antenna, quad-ridge flared horn, measurement, square kilometre array, meerkat.

## I. INTRODUCTION

Large telescope arrays are valuable tools for radio astronomers in the pursuit of high sensitivity observations. For the international project Square Kilometre Array (SKA) [1], construction has now begun of the first 15 m shaped offset Gregorian dual-reflectors [2] for the SKA-MID. The SKA-MID, located in South Africa, will cover frequencies from 350 MHz to 15.3 GHz with multiple feed packages on the indexer for each of these 133 reflectors. As the name suggests, the SKA will offer a square kilometre of total collecting area once finalized. The MeerKAT (“More” Karoo Array Telescope) project, developed and constructed in South Africa, is a precursor to SKA and consists of 64 unshaped offset Gregorian dual-reflectors each with a projected aperture 13.5 m in diameter [3]. MeerKAT was inaugurated in 2018 and will eventually be included in the SKA-MID. The SKA will be the largest and most sensitive telescope for the available frequencies and enable new science possibilities. Another key feature is the possibility of wide continuous bandwidth for observation. This can be achieved with highly optimized wideband systems and at the same time reduce the number of feed packages needed.

The wideband feed package for SKA Band 1, developed at Onsala Space Observatory, covers 350–1050 MHz with a single pixel feed system and is close to being finalized. The first prototype was successfully installed and telescope

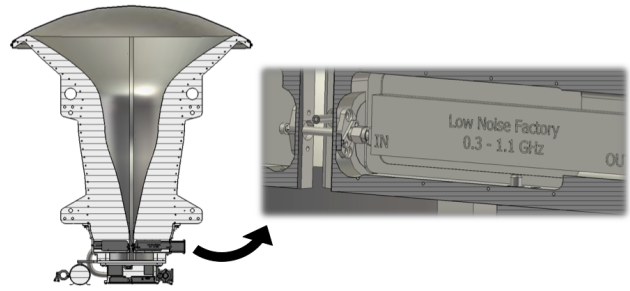


Fig. 1. Cross-section view of the SKA Band 1 feed package.

main beam patterns measured [4] on the Dish Verification Antenna 1 (DVA1) at DRAO in Penticton, Canada in 2016. The 3:1 quad-ridge flared horn (QRFH) feed package is a room temperature system with low-noise amplifiers (LNA) [5] integrated directly inside the horn ridges, removing the need for a cryostat [6]. The horn and ridges were designed from spline-defined profiles where numerical points, connected through splines, define the shape. These points were optimized with genetic algorithm (GA) and particle swarm optimization (PSO). The crucial requirement for the receivers of SKA is the absolute sensitivity level,  $A_{eff}/T_{sys}$ , where  $A_{eff}$  is the effective area of the reflector and  $T_{sys}$  is the total system noise temperature. Therefore, the main optimization goal for the Band 1 feed package was high sensitivity across the band. To estimate sensitivity, a system simulator that applies GRASP physical optics (PO) and physical theory of diffraction (PTD) was used [7].

As part of the qualification tests of the SKA Band 1 feed package, the final prototype was installed and tested on one of the MeerKAT reflector dishes in 2018. In this paper we present the results of those sensitivity tests and compare to simulation. We also present measurements of aperture efficiency and the intrinsic cross-polarization (IXR). Good agreement is found between the measured and simulated results on the MeerKAT dish. This validates the simulation technique which predicts the SKA Band 1 feed package to fulfill the requirements on the SKA reflector dish.

## II. FEED PACKAGE - OVERVIEW

The QRFH is assembled from four plaster-moulded flare-pieces which clamps the four ridges between them and then

connects to the bottom bowl. The ridges and bottom bowl are manufactured using computer numerical control (CNC) machining. At the feeding point of the QRFH, the ridges are hollowed out to mount the single-ended room temperature LNAs [5], supplied by Low Noise Factory (LNF), directly with the  $50 \Omega$  feeding-pin interface, see Fig. 1. Due to the pure metal structure of the QRFH it has low ohmic loss and with the two orthogonal ridge-pairs there is no need for an orthomode transducer (OMT) to achieve dual-linear polarization. The feed aperture is covered with a polycarbonate (PC) radome for environmental protection and a metal shield protects the feed body and electronics box. To prevent moisture condensation, a desiccator is connected to the lower part of the feed. There will be no details given on the electronics system of the feed package in this paper. In Fig. 1 a cross-section of the feed package (without metal shield) is presented. The spline-defined profile of the SKA Band 1 QRFH allows for a customized “curved” shape, tailored for high  $A_{eff}/T_{sys}$  on the SKA reflector. The requirement set for  $S_{11} < -10$  dB across the full bandwidth of 350–1050 MHz, is clearly achieved for both ports in Fig. 2(a). The measured port isolation in Fig. 2(b) deviates from simulated but is better than  $-35$  dB for most of the bandwidth.

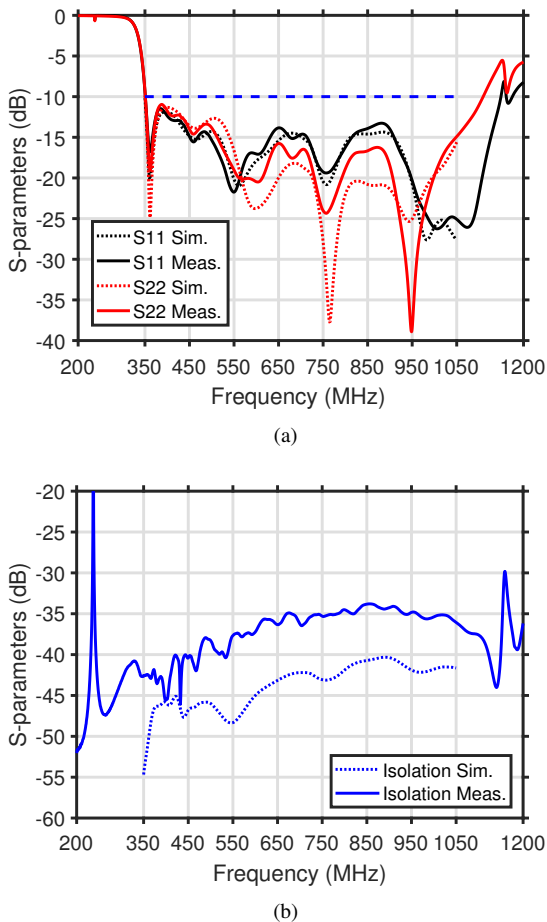


Fig. 2. SKA Band 1 QRFH s-parameters simulated and measured. (a) Input reflection for each port; (b) Isolation between the ports.

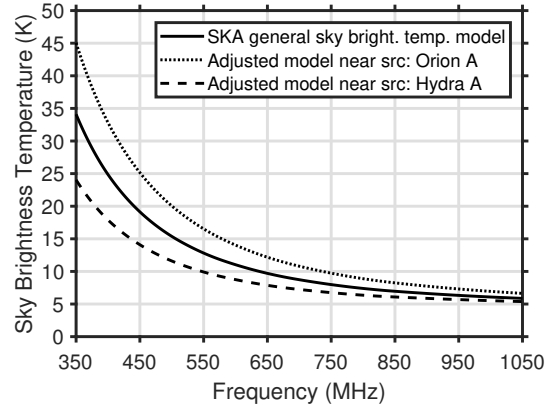


Fig. 3. SKA general sky brightness temperature model used in antenna noise temperature simulation. The additional two curves represent the model adjusted for proximity to sources Orion A and Hydra A in the sky.

### III. SYSTEM SIMULATOR

Simulation of the antenna noise temperature,  $T_a$ , is performed in two steps with the system simulator. First, the reflector model is fed with simulated or measured feed beam patterns from the focal point of the reflector to calculate the reflector beam pattern. The position of the feed is optimized for high phase efficiency on the reflector at the high end of the frequency band. Second, the reflector beam pattern is used to weight the surrounding brightness temperature,  $T_b$ , in a full-sphere integration for each frequency and pointing direction of the telescope according to:

$$T_a = \frac{\int \int_{4\pi} G(\theta, \phi, f) T_b(\theta, \phi, f) \sin \theta d\theta d\phi}{\int \int_{4\pi} G(\theta, \phi, f) \sin \theta d\theta d\phi} \quad (1)$$

$T_b$  is comprised of a sky brightness model above the horizon and a ground noise model below the horizon, and is assumed to be symmetric in azimuth direction. Following SKA standard, the general brightness temperature model given in [8] is here used for  $T_b$ . The sky brightness part of  $T_b$  for Band 1 frequencies can be seen as the solid curve in Fig. 3. The total system noise temperature is given as  $T_{sys} = \eta_{rad} T_a + (1 - \eta_{rad}) T_{phy} + T_{rec}$ , where  $\eta_{rad}$  is the antenna radiation efficiency,  $T_{phy}$  the physical temperature of the antenna and  $T_{rec}$  the receiver noise temperature. In addition a margin of 1-2 K is added to  $T_{sys}$  for noise likely to be caused by the back-end and digitization. During Band 1 design,  $T_{rec}$  was estimated with measurements of the LNAs and the additional feed package components noise contribution. In [4] the receiver noise was measured to confirm this number. The effective area is calculated from the simulated reflector main-beam gain,  $G$ , according to  $A_{eff} = (G\lambda^2)/(4\pi)$ . From these simulations we calculate sensitivity as  $A_{eff}/T_{sys}$ . The pointing direction of the telescope is given in zenith angle,  $\theta_p$ , where  $0^\circ$  represent zenith and a larger  $\theta_p$  means the direction is closer to the horizon.

#### IV. SIMULATION ON SKA DISH

The SKA Band 1 feed package is designed for the SKA dish which is a 15 m shaped offset Gregorian dual-reflector. The half-subtended angle,  $\theta_e$ , from feed towards sub-reflector is  $58^\circ$  with a  $-12$  dB edge-taper. The dish is in *feed-down* configuration which means that the sub-reflector moves towards the ground when observation direction is closer to the horizon. The sub-reflector has a  $40^\circ$  spill-over shield extending down from the edge closest to the ground. This shield significantly reduces the spill-over noise temperature contribution from the ground to  $T_a$ . Simulated results for the Band 1 feed package on the SKA dish is presented in Fig. 4: (a) The sensitivity fulfils the requirement (above dashed blue line) across frequency and zenith angle  $\theta_p \in [0^\circ, 60^\circ]$  for both polarizations; (b) Aperture efficiency,  $\eta_a$ , reaches a minimum of 72 % and maximum 85 % over the band, which is excellent for a 3:1 bandwidth feed; (c) The Band 1 polarization purity on the reflector is given as intrinsic cross-polarization (IXR) [9], and fulfils the requirement of minimum IXR within half-power beamwidth better (more) than 15 dB (dashed blue line). Note that the sensitivity requirement is lower for 350–650 MHz due to significantly higher sky brightness temperature at these frequencies, see Fig. 3.

#### V. SIMULATION AND MEASUREMENT ON MEERKAT DISH

The SKA Band 1 feed package was installed and tested on the MeerKAT unshaped offset Gregorian dual-reflector dish with feed-down configuration, see Fig. 5. The theoretical MeerKAT reflector is 13.5 m in diameter with a spill-over shield extending  $20^\circ$  downward from the sub-reflector. Optimal edge-taper is  $-12$  dB for  $\theta_e = 49^\circ$ . The smaller  $\theta_e$  compared to the SKA dish, results in over-illumination from the SKA Band 1 feed of the MeerKAT sub-reflector and a higher spill-over noise contribution to  $T_a$ . The over-illumination and the fact that the MeerKAT reflector is unshaped, results in lower  $\eta_a$ . The increased spill-over noise, smaller reflector diameter and lower  $\eta_a$  combines to lower expected sensitivity for the SKA Band 1 feed package on the MeerKAT dish than on the SKA dish.

##### A. Sensitivity

There is a difference in effective diameter between the theoretical MeerKAT reflector model used in simulation and the constructed MeerKAT reflector. The constructed MeerKAT reflector has a slightly larger diameter of 13.97 m, due to the tiles extending the area as seen in the top-left of Fig. 5. This results in approximately 7 % larger  $A_{\text{eff}}$  available during sensitivity measurement compared to simulation. Therefore during comparison, the measured data is scaled down by this factor. The theoretical reflector model, seen top-right of Fig. 5, does not account for mechanical framework surrounding the reflector frame and the tiled structure of the reflector. This could influence the reflector beam pattern in terms of scattering the spill-over power.

In Fig. 6 the simulated and measured sensitivity of the SKA Band 1 feed package installed on a MeerKAT reflector

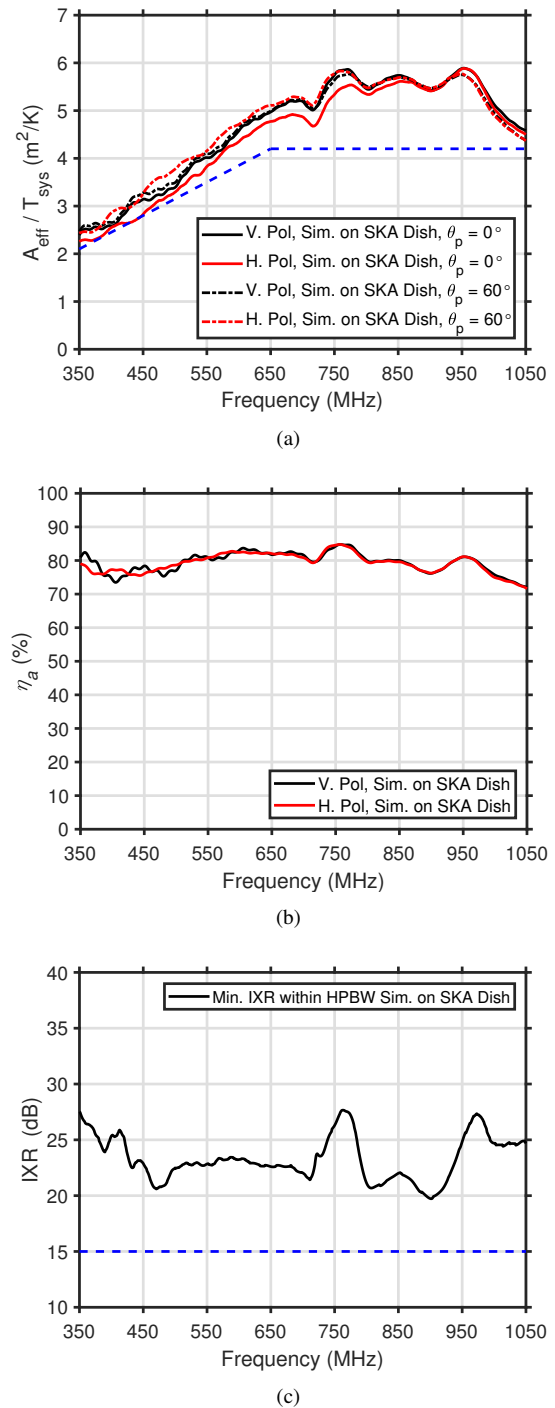


Fig. 4. SKA Band 1 feed package simulated on SKA dish, for both polarizations. (a) Sensitivity given for  $|\theta_p| = 0^\circ$  and  $|\theta_p| = 60^\circ$ ; (b) Aperture efficiency; (c) Minimum IXR within half-power beamwidth.

is presented for three zenith angles available. The error bars adjust for the approximate change in sky brightness temperature near the sources Orion A and Hydra A used for these measurements, see Fig. 3. These adjustments are based on a global sky model extrapolated from Haslam's 408 MHz model [10]. Sensitivity data are determined from  $\sim 1$  hour

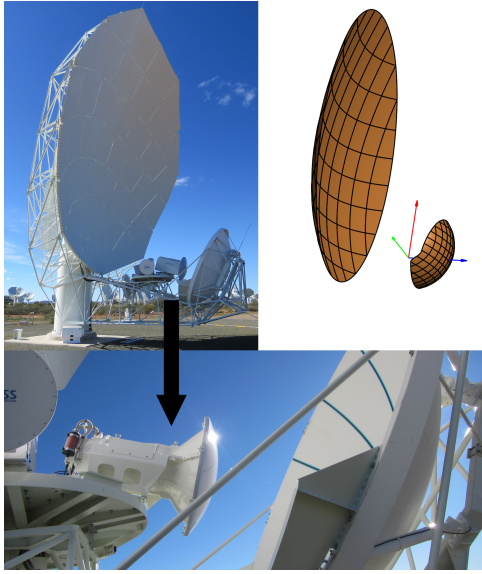
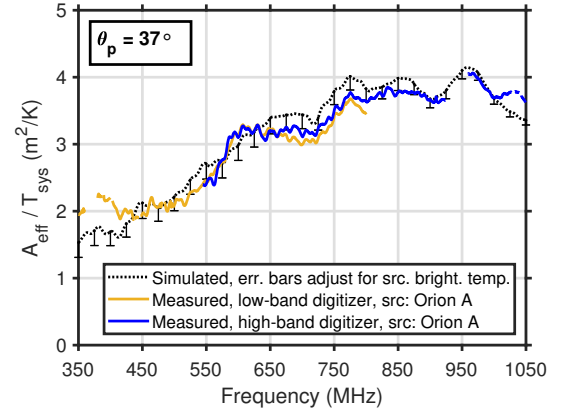


Fig. 5. (Top-left) MeerKAT dish as constructed in South Africa; (Top-right) MeerKAT dish as theoretical simulation model; (Bot.) Zoom-in on the SKA Band 1 feed package mounted during tests (without metal shield) on a MeerKAT dish.

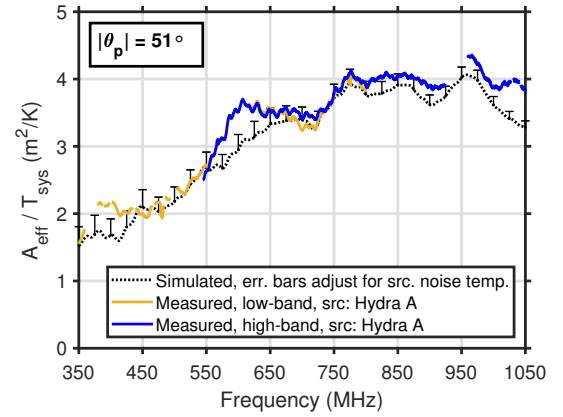
drift scans of these sources with measured system equivalent flux density (SEFD) converted to sensitivity according to  $A_{\text{eff}}/T_{\text{sys}} = 2k_B/\text{SEFD}$  where  $k_B$  is the Boltzmann constant. Measurements were recorded with two different digitizers for the low and high frequency band. Only one polarization is shown here since one LNA malfunctioned during the measurement and produced non-usable data. Radio frequency interference (RFI) has been removed from the measured data and is shown as gaps. With the mentioned corrections for  $A_{\text{eff}}$  and the sky brightness temperature, sensitivity  $A_{\text{eff}}/T_{\text{sys}}$  show good agreement with simulation over the band. At the upper frequency range, the difference is due to lower  $T_{\text{rec}}$  measured ( $< 20$  K) than what was conservatively estimated.

### B. Aperture efficiency and intrinsic cross-polarization (IXR)

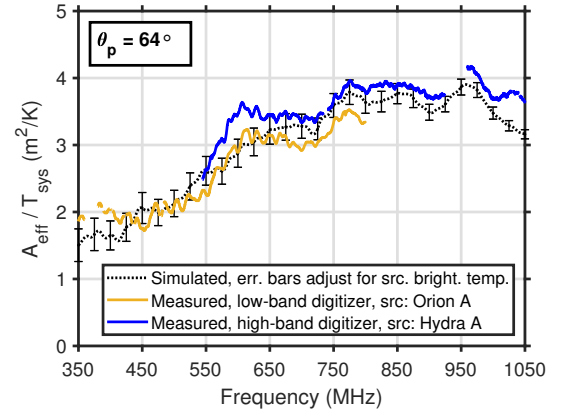
Reflector beam patterns were measured using the unresolved quasar 3C273 which is less than one arcminute in extent on the sky. Microwave holography was implemented using one of the other MeerKAT reflectors as reference. Due to availability of only one digitizer for the low frequency band, beam pattern measurements using this technique could only be performed for the upper range of frequencies. The farfield complex voltage beam pattern measured is transformed to the aperture plane. The aperture efficiency,  $\eta_a$ , is then calculated from the aperture plane complex voltage distribution according to IEEE standard 145. Because a limited solid angle is sampled during this measurement, an over-estimate of the aperture efficiency is produced from the given method. From previous MeerKAT receiver measurements at these frequencies, this over-estimate of  $\eta_a$  has been shown to be in the order of  $\sim 7\%$  over most of the band but drops to  $\sim 3\%$  over the upper band. In Fig. 7(a) we have applied corrections for this over-estimate to



(a)



(b)



(c)

Fig. 6. SKA Band 1 feed package sensitivity on MeerKAT dish, simulated and measured for vertical polarization. Error bars represent the adjustment of the general SKA sky brightness temperature model to account for proximity to the sources used in measurement. Upper and lower error bar in the same figure means two different sources were used for low and high band measurement. Three zenith angles shown: (a)  $\theta_p = 37^\circ$ ; (b)  $\theta_p = 51^\circ$ ; (c)  $\theta_p = 64^\circ$ .

the measured data in form of error bars. With the corrections the measured  $\eta_a$  is in close agreement with simulated data.

IXR is calculated from the Jones-matrix of the reflector

beam patterns. In Fig. 7(b), frequency samples of IXR calculated from measured data are presented and compared to simulations. The measured Jones-matrix was normalized to maximum bore-sight gain for vertical and horizontal polarization respectively in the calculation. There was no measurement to constrain the gain for each polarization which could result in a systematic error of the IXR calculation. This could explain why the measured data show better result compared to simulated.

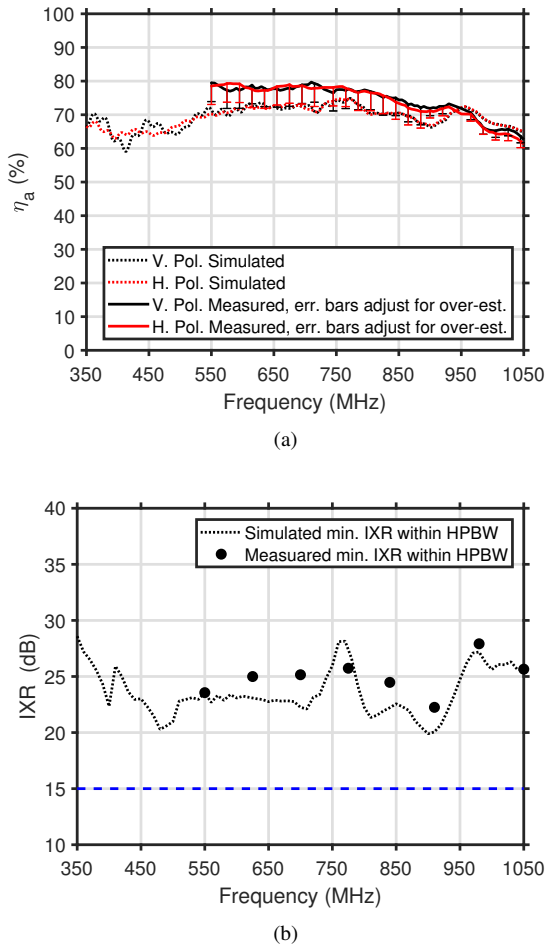


Fig. 7. SKA Band 1 feed package  $\eta_a$  (a) and IXR (b) on MeerKAT dish, simulated and measured. Error bars represent the correction applied to the over-estimation of  $\eta_a$  in the measurement technique. SKA lower-limit requirement on IXR is shown as dashed blue line.

## VI. CONCLUSION

The SKA project is moving into the construction phase of the SKA-MID reflector dishes, which will be equipped with multiple feed packages. The 3:1 QRFH feed package design for SKA Band 1 over 350–1050 MHz is close to being finalized. In this paper, we have presented the first measured sensitivity data of the Band 1 feed package from tests on the SKA precursor reflector MeerKAT. The measured and simulated sensitivity levels agree after appropriate corrections

have been applied. These corrections accommodate for sky brightness temperature near sources used in the sky and the difference in available reflector area between simulated model and the constructed reflector. In addition, good agreement is found between simulated and measured aperture efficiency with an expected 70 % average over the frequency band on a MeerKAT dish. The results validate the confidence in predicted performance of the feed package and the PO+PTD system simulator. Therefore, once the feed package is installed on the SKA dish for which it was designed, it should achieve the SKA requirements. In the near future, the feed package will be tested on the SKA dish, and the measured results will be compared to PO+PTD and full-wave simulations.

## ACKNOWLEDGMENT

This work has been funded by Swedish VR Research Infrastructures Planning Grant Swedish contributions to the SKA radio-telescope in its pre-construction phase. System simulator was provided by M. Ivashina at the Dept. of Electrical Eng., Chalmers University. Thanks to: I. Theron, R. Lehmensiek, and J. Kotze, EMSS Antennas, for guidance and supplying the initial feed model; to SARAO for enabling the MeerKAT tests; to J. Schlee, LNF, for his dedication to the project; to the mechanical workshop at Onsala for all their hard work.

## REFERENCES

- [1] P. E. Dewdney, W. Turner, R. Millenaar, R. McCool, J. Lazio, and T. J. Cornwell, "SKA1 System Baseline Design (SKA-TEL-SKO-DD-001)," Mar. 2013. [Online]. Available: [https://www.skatelescope.org/wp-content/uploads/2012/07/SKA-TEL-SKO-DD-001-1\\_BaselineDesign1.pdf](https://www.skatelescope.org/wp-content/uploads/2012/07/SKA-TEL-SKO-DD-001-1_BaselineDesign1.pdf)
- [2] R. Lehmensiek, I. P. Theron, and D. I. L. de Villiers, "Deriving an Optimum Mapping Function for the SKA-Shaped Offset Gregorian Reflectors," *IEEE Trans. Antennas Propag.*, vol. 63, no. 11, pp. 4658–4666, 2015.
- [3] I. P. Theron, R. Lehmensiek, and D. I. L. de Villiers, "The design of the MeerKAT dish optics," in *Proc. Int. Conf. Electromagn. Advanced Appl. (ICEAA 2012)*, Sep. 2012, pp. 539–542.
- [4] J. Flygare, B. Billade, M. Dahlgren, M. Pantaleev, J. Dahlström, B. Wästberg, G. Hovey, R. Hellyer, R. Messing, B. Veidt, G. Lacy, and M. Islam, "Beam pattern measurement on offset Gregorian reflector mounted with a wideband room temperature receiver for the Square Kilometre Array," in *Proc. IEEE Int. Symp. Antennas Propag. (AP-SURSI 2018)*, Boston, MA, USA, Jul. 2018.
- [5] J. Schlee, N. Wadefalk, P. A. Nilsson, and J. Grahm, "10 K room temperature LNA for SKA band 1," in *IEEE MTT-S Int. Microw. Symp. Dig. (IMS 2016)*, San Francisco, CA, USA, Aug. 2016.
- [6] B. Billade, J. Flygare, M. Dahlgren, B. Wästberg, and M. Pantaleev, "A wide-band feed system for SKA band 1 covering frequencies from 350 - 1050 MHz," in *Proc. 10th Euro. Conf. Antennas Propag. (EuCAP 2016)*, Davos, Switzerland, Apr. 2016.
- [7] M. V. Ivashina, O. Iupikov, R. Maaskant, W. A. Van Cappellen, and T. Oosterloo, "An optimal beamforming strategy for wide-field surveys with phased-array-fed reflector antennas," *IEEE Trans. Antennas Propag.*, vol. 59, no. 6, pp. 1864–1875, 2011.
- [8] G. Cortes-Medellin, "MEMO 95 Antenna noise temperature calculation," pp. 1–13, Jul. 2007. [Online]. Available: [https://www.skatelescope.org/uploaded/6967\\_Memo\\_95.pdf](https://www.skatelescope.org/uploaded/6967_Memo_95.pdf)
- [9] T. D. Carozzi and G. Woan, "A fundamental figure of merit for radio polarimeters," *IEEE Trans. Antennas Propag.*, vol. 59, no. 6, pp. 2058–2065, Jun. 2011.
- [10] A. de Oliveira-Costa, M. Tegmark, B. M. Gaensler, J. Jonas, T. L. Landecker, and P. Reich, "A Model of Diffuse Galactic Radio Emission from 10 MHz to 100 GHz," *Monthly Notices of the Royal Astronomical Society*, vol. 388, pp. 247–260, Jul. 2008.